Nigerian Journal of Technology (NIJOTECH)
Vol. 42, No. 3, September, 2023, pp.330 - 338
www.nijotech.com

Print ISSN: 0331-8443
Electronic ISSN: 2467-8821
https://doi.org/10.4314/njt.v42i3.5

DEVELOPMENT OF A MULTIGENERATION SYSTEM WITH INTEGRATED HYDROGEN PRODUCTION: A TYPICAL ANALYSIS

AUTHORS:
E. Frank[1,*], and S. O. Effiom[1]

AFFILIATIONS:
[1]Department of Mechanical Engineering, Cross River University of Technology, Calabar, Cross River State, Nigeria.

***CORRESPONDING AUTHOR:**
Email: virtuousfrank2012@gmail.com

ARTICLE HISTORY:
Received: 09 February, 2023.
Revised: 08 August, 2023.
Accepted: 17 August, 2023.
Published: 01 November, 2023.

KEYWORDS:
Multigeneration plant, Energy and exergy Efficiencies, Economic modell-ing, PEM Electrolyzer.

ARTICLE INCLUDES:
Peer review

DATA AVAILABILITY:
On request from author(s)

EDITOR:
Ozoemena Anthony Ani

FUNDING:
None

Abstract

Rise in demand for energy and emission from fossil fuels has become a thing of concern to researchers and Engineers. It is one thing to provide the energy needed by the society, and another to produce a clean and eco-friendly power supply. In this study, a thermodynamic and economic modelling of a solar-driven multigeneration power plant (MGPP) integrated with a PEM Electrolyzer for hydrogen production is examined. The performance indicators considered include energy and exergy efficiencies, net work, energetic and exergetic COP, cooling rate. Results of the thermodynamic analysis show that the energy and exergy efficiencies excluding the fuel cell was 28.57% and 34.79% respectively; when the fuel cell was incorporated, the energy and exergy efficiencies were respectively 24.45% and 34.63%. The energetic and exegetic COP was 0.609 and 0.281 respectively. Additionally, net work, cooling rate, and hydrogen production were respectively 52.75kW, 86.83kW, and 0.0114kg/s. The economic analysis indicates a unit cost of electricity (UCOE) at $0.025/kWh, a life cycle cost of $0.1097 and a payback period of 4years was achieved. The developed multigeneration system is technically and economically viable with net zero CO_2 emissions. It can also serve as an alternative option to fossil-powered plants and sectors with less energy demand.

1.0 INTRODUCTION

One of the indicators of industrialization and economic progress, and sustainable development is energy accessibility. Following the global projection to about seven billion, energy demand is expected to increase [1]. The increasing energy demand as well as the declining fossil fuels energy resources have triggered researchers to evolving other proficient energy transformation systems called multigeneration systems (MGS) and likewise finding substitutes to conventional fossil-fuels. Apart from monitoring the environmental complications and cost, MGS have an extraordinary capacity to improve environmental sustainability and augment efficiency [2]. Several academics have offered the application of MGS for power generation. For example, [3] evaluated the thermodynamic performance of an integrated solar-biomass hybrid system for heating and power-cooling production. The work shows a high prospective for the solar-biomass MGS. The thermal efficiency and the economic valuation of a natural-gas-fired plant for mutual energy production was examined by [4]. The study showed an enhancement in energy efficiency calculated at 82% with a decrease in CO_2 emissions of nearly 51.5%. Also, a solar-geothermal multigenera-

HOW TO CITE:
Frank, E., and Effiom, S. O. "Development of a Multigeneration System with Integrated Hydrogen Production: A Typical Analysis", *Nigerian Journal of Technology*, 2023; 42(3), pp. 330 – 338; https://doi.org/10.4314/njt.v42i3.5

tion system and solar-driven tri-generation plants were proposed by [5]. In the proposed plant, the geothermal-solar plant was nominated for power generation, hot water production, space heating, cooling and heat. In contrast, the solar-driven trigeneration plant was for electricity power generation and space heating. The dual thermal plants reached an exergy efficiency not greater than 36.6% and 24. 66%, respectively.

Furthermore, hydrogen production in recent times has been one of the products in several MGS. Hydrogen (H_2) is considered a future fuel to the global economy because of its eco-friendly capacity and cheap production method. For instance, several methods, which include steam methane reforming, splitting water via photocatalyst, biomass conversion process, Electrolyzer and thermochemical cycles, have been applied to produce H_2 [6]. Other studies on MGSs, which comprise hydrogen production, are establish in the study of [7]. Their system achieved 43% and 65% for energy and exergy efficiencies respectively. The maximum generated power was calculated at 48kW. Also, the cooling capacity was sustained at 28kW, heating 298.5kW and overall CO_2 savings were estimated at 1614 tons of CO_2/year. The present study, thus, is to provide a comprehensive review of current research boundaries and developed a multigeneration plant for power, cooling, heating and hydrogen production with an extended fuel-cell at the bottoming cycle for domestic energy resource. The developed MGS is solar-driven using the localized solar irradiance, followed by thermodynamic and economic evaluation.

From the reviewed literature, conventional power generating turbines can achieve efficiencies up to 60 and 70% for plant capacity of about 100kW**.** Also, the reviewed studies show that multigeneration power cycles and hydrogen production are promising technology to tackle environmental complexities. Nevertheless, adequate experimental studies are needed to authenticate the investigative assumptions. Thus, different cycle's performance must be compared based on reliable definitions of performance indices**.** Secondly, a number of the studies reviewed, show that waste heat recovered emanates from a topping gas turbine plant, engine-based or solar thermal plant have been employed to produce heat, supplementary power, cooling and hydrogen production in the bottoming cycles. The components configurations are critical for satisfactory utilization of the energy source, economics and environmental sustainability. In this study, the system's components are reduced and an additionally fuel cell unit is integrated to sustain power supply due to uncertainties that may exist from solar irradiance fluctuation. Thirdly, studies regarding the solar potential for Calabar in this respect is not common in open literature. Specific data is generated for long term energy projection aid and some policies for deep decarbonization pathways and as a contribution to Nigeria's energy plan.

2.0 METHODOLOGY

2.1 Materials

Daily data on the solar irradiance in Calabar for a period of ten years was obtained from Nigeria Meteorological Centre, Calabar. The average data is used as a basis for choosing simulation data for the proposed MGS and the sub-system of the plant. Additionally, the system modelling was done using Engineering Equation Solver (EES), while secondary data is obtained from open literature and scientific documents made public. Other simulation parameters that may be required based on assumptions include: solar beam irradiation, collector aperture area, volumetric flow rate on the parabolic trough solar collector, receiver inner diameter, receiver outside diameter, working fluid selection, isentropic efficiency of turbine, and isentropic efficiency of pump.

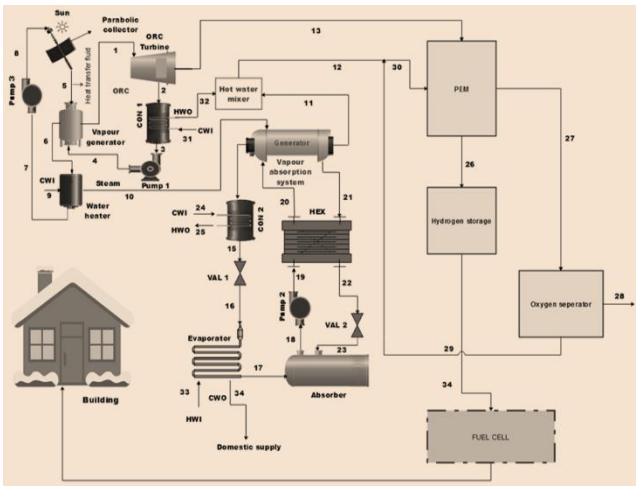

Figure 1: Proposed solar-driven ORC and vapour absorption integrated system

2.2 System Description

The proposed solar-driven combined system is shown in Figure 1. It system encompasses four subsystems which combine to offer the four products namely; cooling, heating, power and hydrogen production. The topping unit is a solar unit, which powers an ORC. Heat from the sun is absorbed by the parabolic collector. The fluid at high temperature flows to the vapour generator (VG) causing the refrigerant (R245fa) in the VG to boil and expand. The expanded fluid enters the ORC turbine at state 1, producing shaft

work and electricity at state 13. Furthermore, the fluid enters the condenser at state 2 and exit at state 3 as saturated liquid. The liquid is pumped to the VG at state 4 to repeat the ORC cycle. Similarly, part of the heat from the VG is used to produce steam at state 10 while the hot fluid returns to the receiver to be reheated. The steam produced is used to power the generator in the VAS (vapour absorption system) to produced refrigerating effect in the evaporator at state 16. The exiting steam from the generator at state 11 and the hot water from condenser 1 at state 32 enters the hot water mixer to produce a single-phase condition. The exiting hot water at state 12 mixed with the hot water from the Oxygen separator entering as hot water to the PEM at state 30 to enhance the hydrogen production. The hydrogen produced is further used to power a fuel cell for continuous electricity production. The bottoming subsystem which is the absorption cooling and heating system is used to provide both cooling and heating loads. The heat input to the absorption system is provided by the steam generated from the water heater at state 10.

2.3 Thermodynamic Modelling

The mass and energy balance of the system is based on the steady state process and conservation of mass as assumed for this analysis. The steady state energy and conservation equations are presented as in [8].

$$\sum_i m_i = \sum_j m_j \quad (1)$$

$$\sum \dot{Q} - \sum \dot{W} = \sum m_j h_j - \sum m_i h_i \quad (2)$$

The energy balancing of the component system for the integrated system is based on Equations (1) and (2). The analysis of the parabolic solar collector (PSC) is presented based on [9].

2.4 Energy of the Parabolic Collector

The useful energy, which is the amount of energy gained by the solar collector can be evaluated from:

$$\dot{Q}_{u=\mathrm{F_R}}\mathrm{R}[S_{col} \times A_a - A_r U_L(T_{in} - T_{amb})] \quad (3)$$

The rate of solar energy delivered from the concentrated solar collector is obtained as:

$$Q_{sol} = A_a S_{col}(Col_r) \quad (4)$$

Where: A_a, S_{col}, A_r, Col_r, F_R, and U_L connotes the aperture area (m^2), Solar Absorptivity (W/m^2), area of receiver (m^2), number of collectors in rows, heat removal factor, and overall heat loss coefficient respectively.

2.5 Exergy Modelling of the Component System

Following the general exergy balance expression:

$$\sum e_{ij} = \sum e_{x,out} + e_D \quad (5)$$

Where; $e_x = \Delta h - T_0$ (6)

The exergy balance efficiencies of components of the system is presented in Table 1.

2.6 Performance Indicators

The following indicators have been considered in order to examine the thermodynamic performance of the proposed MGS.

2.6.1 Thermal efficiency

The Thermal efficiency (energy efficiency) of the proposed MGS without fuel cell η_{th_1} is adopted from that presented by [10] and is given as;

$$\eta_{th} = \frac{\dot{W}_{net} + m_{32}h_{32} - m_{31}h_{31} + \dot{m}_{H_2} \times LHV_{H_2} + Q_{Eva} + \dot{Q}_{WH} + \dot{W}_{PEM}}{Q_{PTSC}} \quad (7)$$

Where $\dot{W}_{net}, \dot{Q}_{WH}, \dot{m}_{H_2}, LHV_{H_2}, Q_{Eva}, Q_{PTSC}$ is the network produced by the ORC sub system, heat generated by water heater, mass flow rate, Lower heating value of hydrogen, refrigerating effect and overall heat input to the system respectively.

The overall energy efficiency of the proposed MGS with fuel cell (η_{th_2}) is given as;

$$\eta_{th_{F,C}} = \frac{\dot{W}_{net} + m_{32}h_{32} - m_{31}h_{31} + \dot{Q}_{WH} + W_{fuelcell} + Q_{Eva} + \dot{W}_{PEM}}{Q_{PTSC}} \quad (8)$$

where; $W_{fuelcell}$ = work done by fuel cell

2.6.2 Exergy efficiency

The exergy efficiency of the system without fuel cell is given as;

$$\eta_{ex} = \frac{\dot{W}_{net} + \dot{E}_{H_2} + \dot{E}_{Eva} + \dot{m}_{32}h_{32} - \dot{m}_{31}h_{31} + Ex_{H_2} + Ex_{WH} + W_{PEM}}{\dot{E}x_{PTSC}} \quad (9)$$

The exergy efficiency of the system including the fuel cell is given as;

$$\eta_{ex_{F,C}} = \frac{\dot{W}_{net} + \dot{E}_{H_2} + \dot{E}_{Eva} + \dot{m}_{32}h_{32} - \dot{m}_{31}h_{31} + Ex_{H_2} + Ex_{WH} + W_{PEM}}{\dot{E}x_{PTSC}} \quad (10)$$

Table 1: Exergy balances and Efficiencies of component of the proposed MGPP

Component	Exergy balance	Exergy of fuel	Exergy of prod.	Exergy efficiency
PTSC	$\dot{E}x_8 = \dot{E}x_5 + E_{solar}$	$\dot{E}x_8 - \dot{E}_5$	$\dot{E}_{solar}$	$\frac{\dot{E}x_8 - \dot{E}_5}{\dot{E}_{solar}}$
ORC turbine	$\dot{E}x_1 = \dot{E}x_2 + \dot{W}_{ORCTURB} + E_{DTURB}$	$\dot{E}x_1 - \dot{E}_2$	$\dot{W}_{ORCTURB}$	$\frac{\dot{W}_{ORCTURB}}{\dot{E}x_1 - \dot{E}_2}$

ORC condenser	$\dot{E}x_2 + \dot{E}x_{31} = \dot{E}x_3 + \dot{E}x_{32} + E_{D,CON1}$	$\dot{E}x_2 - \dot{E}x_3$	$\dot{E}x_{32} - \dot{E}x_{31}$	$\frac{(\dot{E}x_{32} - \dot{E}x_{31})}{(\dot{E}x_2 - \dot{E}x_3)}$
ORC vapour generator	$\dot{E}x_4 + \dot{E}x_5 = \dot{E}x_1 + \dot{E}x_6 + E_{DVG}$	$\dot{E}x_5 - \dot{E}x_6$	$\dot{E}x_1 - \dot{E}x_4$	$\frac{(\dot{E}x_1 - \dot{E}x_4)}{(\dot{E}x_5 - \dot{E}x_6)}$
ORC Pump 1	$\dot{E}x_3 + \dot{W}_{ORCPUMP} = \dot{E}x_4 + E_{D,ORCPUMP}$	$\dot{W}_{ORCPUMP}$	$\dot{E}x_4 - \dot{E}x_3$	$\frac{\dot{E}x_4 - \dot{E}x_3}{\dot{W}_{ORCPUMP}}$
VAS generator	$\dot{E}x_{10} + \dot{E}x_{20} = \dot{E}x_{11} + \dot{E}x_{14} + \dot{E}x_{21} + E_{D,GEN}$	$\dot{E}x_{10} - \dot{E}x_{11} + \dot{E}x_{20}$	$\dot{E}x_{14} + \dot{E}x_{21}$	$\frac{\dot{E}x_{14} + \dot{E}x_{21}}{\dot{E}x_{10} - \dot{E}x_{11} + \dot{E}x_{20}}$
VAS condenser 2	$\dot{E}x_{14} + \dot{E}x_{24} = \dot{E}x_{15} + \dot{E}x_{25} + E_{D,CON2}$	$\dot{E}x_{14} - \dot{E}x_{15}$	$\dot{E}x_{25} - \dot{E}x_{24}$	$\frac{(\dot{E}x_{25} - \dot{E}x_{24})}{(\dot{E}x_{14} - \dot{E}x_{15})}$
VAS Pump 2	$\dot{E}x_{18} + \dot{W}_{VASPUMP} = \dot{E}x_{19} + E_{D,VASP}$	$\dot{W}_{VASPUMP}$	$\dot{E}x_{19} - \dot{E}x_{18}$	$\frac{\dot{E}x_{19} - \dot{E}x_{18}}{\dot{W}_{VASPUMP}}$
Pump 3	$\dot{E}x_7 + \dot{w}_{RCPump} = \dot{E}x_8 + E_{D,RCP}$	$\dot{w}_{RCPump}$	$\dot{E}x_8 - \dot{E}x_7$	$\frac{\dot{E}x_8 - \dot{E}x_7}{\dot{w}_{RCPump}}$
Water heater (WHT)	$\dot{E}x_6 + \dot{E}x_9 = \dot{E}x_7 + \dot{E}x_{10} + E_{D,WHT}$	$\dot{E}x_6 - \dot{E}x_7$	$\dot{E}x_{10} - \dot{E}x_9$	$\frac{(\dot{E}x_{10} - \dot{E}x_9)}{(\dot{E}x_6 - \dot{E}x_7)}$
VAS Heat exchanger	$\dot{E}x_{19} + \dot{E}x_{21} = \dot{E}x_{20} + \dot{E}x_{22} + E_{D,HEX}$	$\dot{E}x_{19} - \dot{E}x_{20}$	$\dot{E}x_{22} + \dot{E}x_{21}$	$\frac{\dot{E}x_{22} + \dot{E}x_{21}}{\dot{E}x_{19} - \dot{E}x_{20}}$
Valve 1(Val 1)	$\dot{E}x_{15} + \dot{W}_{Val\,1} = \dot{E}x_{16} + E_{D,Val\,1}$	$\dot{W}_{Val\,1}$	$\dot{E}x_{16} - \dot{E}x_{15}$	$\frac{\dot{E}x_{16} - \dot{E}x_{15}}{\dot{W}_{Val\,1}}$
Valve 2(Val 2)	$\dot{E}x_{22} + \dot{W}_{Val\,2} = \dot{E}x_{23} + E_{D,Val\,2}$	$\dot{W}_{Val\,2}$	$\dot{E}x_{23} - \dot{E}x_{22}$	$\frac{\dot{E}x_{23} - \dot{E}x_{22}}{\dot{W}_{Val\,2}}$
Absorber	$\dot{E}x_{17} + \dot{E}x_{23} + \dot{E}x_{35} = \dot{E}x_{18} + \dot{E}x_{36} + E_{D,Abs}$	$\dot{E}x_{17} + \dot{E}x_{23}$	$\dot{E}x_{18} + \dot{E}x_{36} - \dot{E}x_{35}$	$\frac{\dot{E}x_{17} + \dot{E}x_{23}}{\dot{E}x_{18} + \dot{E}x_{36} - \dot{E}x_{35}}$
Evaporator	$\dot{E}x_{16} + \dot{E}x_{33} = \dot{E}x_{17} + \dot{E}x_{34} + E_{D,Evap}$	$\dot{E}x_{16} - \dot{E}x_{17}$	$\dot{E}x_{33} + \dot{E}x_{34}$	$\frac{\dot{E}x_{33} + \dot{E}x_{34}}{\dot{E}x_{16} - \dot{E}x_{17}}$

2.7 PEM Energy Modelling

The duty of the PEM Electrolyzer in this MGPP is hydrogen production. As shown in Figure 1, electricity and heat are supplied to the Electrolyzer to perform the electrochemical reactions needed. A chemical reaction takes place and hydrogen is separated from water. The remaining water is returned back to the water supply stream for the next hydrogen production cycle.

The total energy demand for PEM electrolysis is obtained from the relationship in [11];

$$\Delta H = \Delta G + T\Delta S \quad (11)$$

Where $T\Delta S$ is the thermal energy demand (J/mol H_2), and ΔG is the electrical energy demand which refers to the change in Gibb's free energy (J/mol. H_2), with values obtained for hydrogen, oxygen and water in [11].

The outlet flow rate of hydrogen is expressed as follows [11];

$$\dot{N}_{H_2} = {}^{J}/_{2F} = \dot{N}_{H_2O,reacted} \quad (12)$$

Where J is the current density and F is Faraday's constant. $\dot{N}_{H_2O\,reacted}$ refer to the reacted water during the electrolysis process.

The rate of water and oxygen at the PEM Electrolyzer outlet are calculated as [12]:

$$\dot{N}_{O_2,out} = {}^{J}/_{4F} \quad (13)$$

$$\dot{N}_{H_2O,out} = \dot{N}_{H_2O,in} - {}^{J}/_{2F} \quad (14)$$

2.8 Economic Analysis

The feasibility of developing and implementing any power plant depends on the economic importance. In this study the feasibility of implementing the proposed multigeneration power plant is evaluated by calculating the total cost rate of the proposed MGPP, using the model equations developed by [13]; [14]; [15] and [16].

Table 2: Equipment Capital Cost

Component	Cost function ($)
PTSC	4500
ORC Turbine	$4750(\dot{W}_{ORCTURB})^{0.85}$
ORC Condenser	$516.6(A_{ORCCOND})^{0.6}$
ORC Pump	$200(W_{ORCPump})^{0.65}$
ORC Vapour Generator	$309.14(A_{ORCVG})^{0.85}$
Water Heater	$0.3m_9$
PEM Electrolyzer	$1000\dot{W}_{PEM}$
VAS Vapour Generator	$130\left(\frac{A_{VASVG}}{0.093}\right)^{0.78}$
VAS Condenser	$1773\dot{m}_{ref}$
VAS Evaporator	$130(\frac{A_{VASEVA}}{0.093})^{0.78}$
VAS Absorber	$130\left(\frac{A_{VASABS}}{0.093}\right)^{0.78}$
VAS Pump	$400\left(\frac{\dot{W}_{VASpump}}{100}\right)^{0.26}$
VAS Solution heat exchanger	$(\frac{A_{VASHEX}}{A_R})^{0.6}$
VAS Throttle valves	$37(\frac{P_{in}}{P_{out}})^{0.68}$

$A_{R=100m^2}$ source: [17]; [18]; [19]

2.8.1 Equipment cost

The purchased equipment cost (PEC) of the system's component is summarized in Table 2. The total cost of the equipment C_{tot} is determined by adding the annual capital cost (ANCC) and the total annual operation cost (ANOC).

C_{tot} = ANCC + ANOC (15)

ANCC = $TIC \times CRF$

$$CRF = \frac{IR\times(1+IR)^n}{(1+IR)^n-1} \quad (16)$$

Where IR, n is interest rate and is set at 0.9% , and life span of the plant and is set at 25years [17].

2.8.2 Operation and maintenance cost

The annual operating cost (ANOC) of the system is gotten by summing up all the operation cost equation (17).

$$ANOC = C_{Labour} + C_{ins,M} + C_{elect} \quad (17)$$

Where, $C_{Labour}, C_{ins,M}, C_{elect}$ = cost of labour, insurance and maintenance cost, and cost of electrical work respectively.

The unit cost of electricity, UCOE($/kWh) is calculated as;

$$UCOE = [C_{tot} + C_{PTSC}] \times \frac{CRF\times\emptyset}{N\times8760} \quad (18)$$

3.0 RESULT AND DISCUSSION

In this study, thermodynamic and economic assessment of a solar power multigeneration system for production of hydrogen, electricity, heating, and cooling was investigated based on energy and exergy analyses. The Engineering Equation Solver (EES) was used to write the codes for modeling the system with respect to balance equations and performance indicators. Parameters of the thermodynamic state points are depicted in Table 3. From the result obtained, the plant equipment cost is low ($0.1945) with a unit cost of electricity at $0.025/kWh.as compared to the current Nigeria electricity tariff which is $0.10/kWh. The hydrogen produced is not used to generate electricity, but is used as an alternative power supply when needed due to some uncertainties in solar irradiation. So, the overall energy and exergy efficiencies of the system excluding the work of the fuel cell are 28.57% and 34.63% respectively. When the fuel cell is incorporated, the energy and exergy efficiencies are respectively 24.45% and 34.63%.

3.1 Variation in Thermodynamic Properties

3.1.1 Effect of turbine inlet pressure on energy and exergy efficiencies

Figure 2(a) shows variation in turbine inlet pressure. It is observed that by increasing the turbine inlet pressure from 500kpa to 800kpa, the overall energy efficiency of the MGPP without fuel cell decreases slightly from 28.29% to 28.16% This is because an increase in pressure ratio requires high compression work and high mechanical irreversibility, thereby causing a reduction in energy efficiency. Similarly, when the fuel cell is incorporated the energy efficiency decreases from 25.6% to 25.47%. However, the overall exergy efficiency increases by 12.5% without fuel cell and by 12.2% with fuel cell. This is due to the fact that the exergy input into the system increases as the pressure ratio increases thus increasing the system's exergy efficiency.

3.1.2 Effect of turbine inlet pressure on power output and exergy destruction

The effect of turbine inlet pressure on power output and the irreversibility in the multigeneration system are shown in Figure 2(b). It was observed that increase in turbine inlet pressure from 500kpa to 800kpa at a constant inlet temperature of 423K leads to increase in power output from 52.75kW to 70.98kW . This is due to the fact that enthalpy drop across the turbine increases as the pressure ratio increases, thereby causing an increase in the power output. Additionally, as the power output increases, the irreversibility in the multigeneration system decreases by 9%.

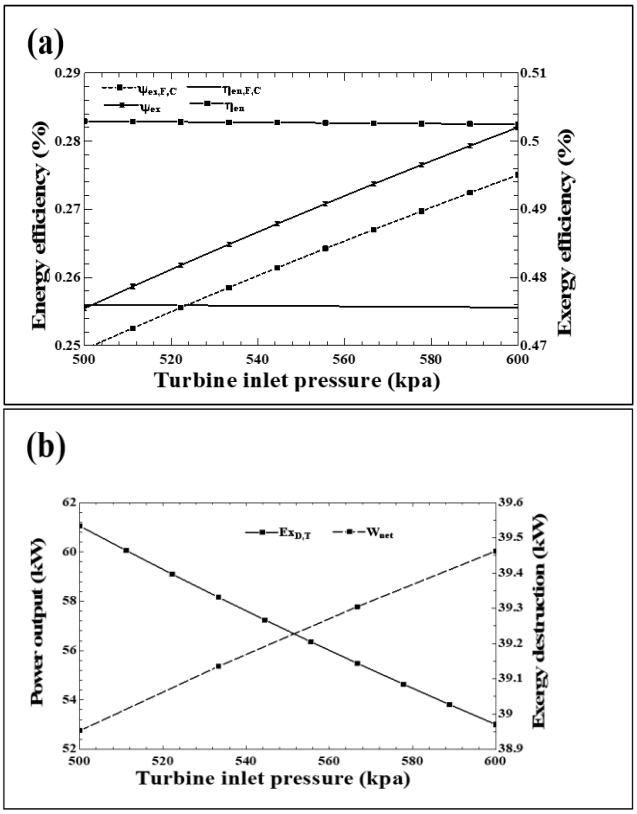

Figure 2: Effect of turbine inlet pressure on (a) energy and exergy efficiencies, (b) power output and exergy destruction

3.1.2 Effect of turbine inlet temperature on energy and exergy efficiencies

Figure 3(a) shows the effect of turbine inlet temperature on energy and exergy efficiencies. It was observed that, as the source temperature increased, there is a greater amount of heat exchange in the ORC vapour generator leading to an increase in the turbine inlet temperature at constant pressure of 500kpa. The increase in temperature leads to an increase in the fluid energy content (enthalpy) thereby increasing the system's efficiencies. The energy efficiency of the MGPP without the fuel cell is increased from 28.57% to 30.22% for turbine inlet temperature mass flow rate of 1.8kg/s. Similarly, the increase in the trend of energy efficiency with fuel cell is the same but the energy values are small. The result indicate that the system decreases in performance with addition of the fuel cell. On the other hand, the exergy efficiency of the system increases from 34.79% to 40.94% for exergy efficiency without fuel cell and that with fuel cell increases by 15%.

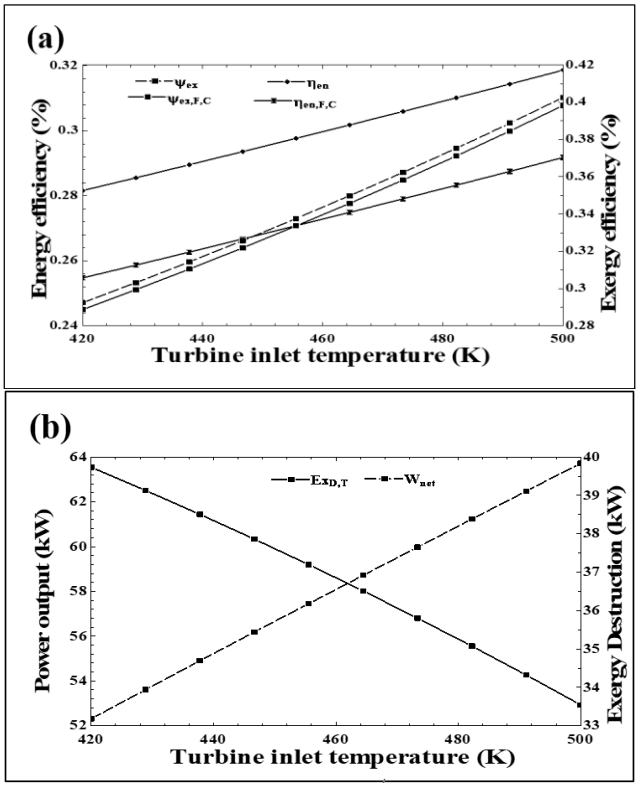

Figure 3: Effect of turbine inlet temperature on (a) energy and exergy efficiencies, (b) power output and exergy destruction

3.1.3 Effect of turbine inlet temperature on power output and exergy destruction

In Figure 3(b), as the turbine inlet temperature is increased from 423K to 470K at a constant pressure of 500kpa and mass flow rate of 1.8kg/s the net power output increases linearly from 52.75kW to 70.98kW. On the other hand, the total exergy destruction of the overall system decreases by 9.4%. This is due to the fact that increasing inlet steam temperature of turbine increases power output nd as such exergy destruction rate reduces leading to a high exergy performance of the overall system.

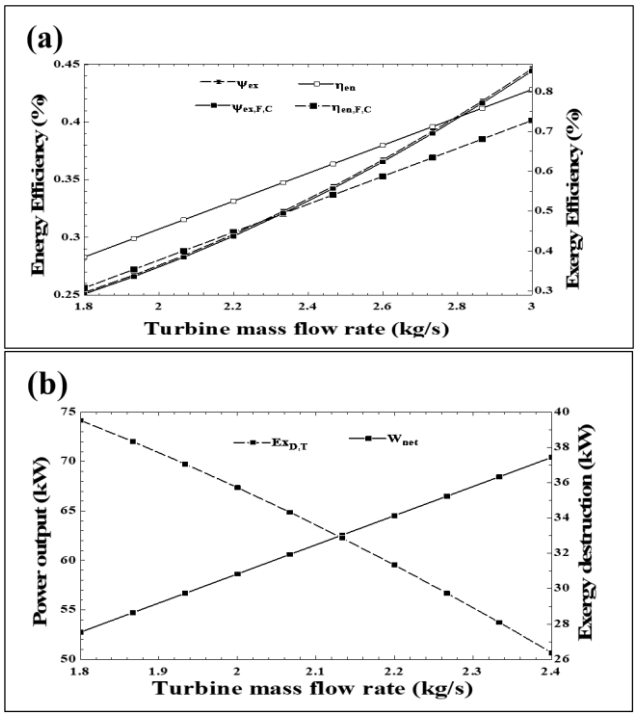

Figure 4: Effect of turbine mass flow rate on (a) energy and exergy efficiencies, (b) power output and exergy destruction

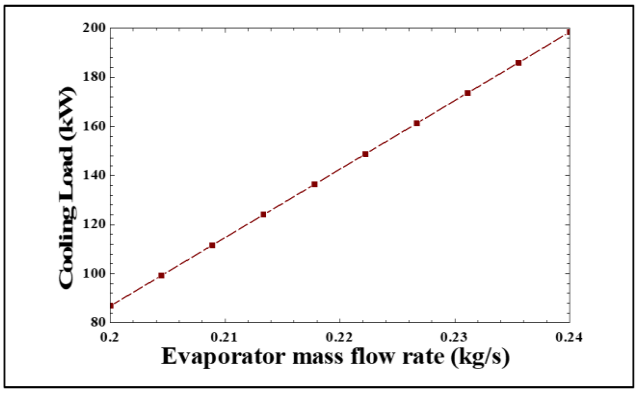

Figure 5: Effect of evaporator mass flow rate on cooling load

3.1.4 Effect of turbine mass flow rate on energy and exergy efficiencies

Figure 4(a) presents the effect of turbine mass flow rate on energy and exergy efficiencies of the overall system without fuel cell and with fuel cell. The energy efficiency without fuel cell increases linearly from 0.28 (28%) to 0.36 (36%) for mass flow rate between 1.8 and 2.4kg/s. the result also shows for 0.07kg/s

mass flow rate increase. The energy efficiency without fuel cell increases by 0.8%.

Similarly, the energy efficiency with fuel cell is the same but the values are small. The increase in efficiency is directly related to the relation between mass flow rate and efficiency in equation 3.26 and 3.28. with constant enthalpy drop. It is important to note that, at higher mass flow rates, temperature drop across the turbine increases, thereby leading to higher efficiency levels at constant pressure.

3.1.5 Effect of turbine mass flow rate on power output and exergy destruction

In Figure 4(b), increasing the turbine mass flow rate from 1.8kg/s to 2.4kg/s produces better rate of heat generated. As a result, net power output increases from 52.75kW at 1.8kg/s to 70.42kW at 2.4kg/s. Increase in mass flow rate leads to increase in turbine work at constant enthalpy triggering an increase in net power production. On the other hand, when the mass flow rate increases from 1.8kg/s to 2.4kg/s, the exergy destruction in the overall system decreases from 39.53kW to 26.37kW due to increase in system's performance.

3.1.6 Effect of evaporator mass flow rate on cooling load

Figure 5 present the effect of evaporator mass flow rate on cooling rate. As can be seen, when the evaporator mass flow rate is increased from 0.2kg/s to 1kg/s the cooling rate increases linearly by 60%. This is due to the fact that increasing the evaporator mass flow rate results in higher cooling generation.

3.2 Validation of Results

The multigeneration power plant was validated and the result compared with that of biomass-based integrated poly-generation power plant as presented in Table 4. Base on energy and exergy efficiency, validated result compared conveniently with that presented in the literature though there were some variations in the present study. This could be attributed to fuel source, heating value of working fluid, and difference in plant configuration. Nevertheless, the energy efficiency of current study's performance is greater than previous study.

Table 3: Thermodynamic Properties of the state points for the combined multigeneration system

State point	Temperature (K)	Pressure (kpa)	Mass flow rate (kg/s)	Enthalpy (kJ/kg)	Entropy (kJ/kg.)K	Exergy (kJ/kg)
1	423	500	1.8	544.5	2.019	87.48
2	392	150	1.8	515	2.019	34.46
3	298	150	1.8	232.3	1.113	11.85
4	298.1	500	1.8	232.5	1.113	12.32
5	453	151.3	2.334	505.9	1.425	200.3
6	403	101.3	2.334	356.9	1.077	94.9
7	348	101.3	2.334	206.3	0.6761	22
8	348	151.3	2.334	206.3	0.6761	22.09
9	293	101.3	1.119	83.3	0.294	0.1986
10	368	101.3	1.119	397.4	1.248	33.42
11	338	101.3	1.119	271.5	0.8916	11.54
12	326.2	101.3	5.176	222.3	0.7435	27.26
13	-	-	-	-	-	-
14	353	7.905	0.2	2649	8.451	27.03
15	314.4	7.905	0.2	172.9	0.5895	0.3473
16	278	0.8635	0.2	172.9	0.6226	-1.626
17	278	0.8635	0.2	2509	9.027	-35.25
18	308	0.8635	7.265	85.03	0.2103	2.095
19	308	7.905	7.265	85.06	0.2103	2.324
20	337	7.905	7.265	144.1	0.3939	33.93
21	353	7.905	7.065	181.8	0.476	63.84
22	318	7.905	7.065	111.3	0.2657	2.072
23	308	0.8635	7.065	91.52	0.2024	8.386
24	298	101.3	3.383	104.2	0.3648	0
25	333	101.3	3.383	250.6	0.8293	26.99
26	326.2	101.3	0.02298	4335	54.67	0.4157
27	326.2	101.3	0.02298	222.3	0.7435	0.121
28	326.2	101.3	0.1824	25.58	0.0822	0.2109
29	326.2	101.3	0.1824	222.3	0.7435	0.9607
30	326.2	101.3	5.176	222.3	0.7435	27.26
31	293	101.3	4.056	83.3	0.294	0.7198
32	323	101.3	4.056	208.8	0.7018	16.85
33	298	101.3	27.37	298.4	5.695	0
34	281	101.3	27.37	281.3	5.636	13.86
35	293	101.3	3.77	83.3	0.294	0.669

36	323	101.3	3.77	208.8	0.7018	15.66

Table 4: Result validation with integrated multigeneration system

Study	References	Energy efficiency	Exergy efficiency	Energetic ORC efficiency	Exegetic ORC efficiency
Technoeconomic assessment of a solar-geothermal multigeneration system for buildings, International journal of hydrogen energy	[6]	17.4	16.6	20.2	49.8
Thermodynamic and Economic modelling of a solar-driven Multigeneration plant integrated with PEM Electrolyzer for hydrogen production	Present study	18.42	37.62	32.75	91.2

4.0 CONCLUSION AND RECOMMENDATION

This research work highlights the potential of solar energy in Calabar. It also provides solutions to clean energy access, environmental sustainability and economic development while attaining reduced GHG emissions. From the study, the MGPP performs optimally within the area of study - Calabar with an average temperature of 29^{o}C and a solar irradiation of 400W/m^2 and a unit cost of electricity (UCOE) of $0.025/kWh as compared to the current tariff of electricity in Nigeria which is $0.10/kWh. The hydrogen production does not interfere with the efficiency of the system, but serve as a fuel for the fuel cell which serves as an alternative power supply during peak periods. In our country like Nigeria and other developing countries of the world with their vast reserve of oil and gas, demand in electricity outweighs power supply due to inadequate or low power generating plants that depend on fossil fuels. The proposed MGPP in this study depend solely on solar energy to generate not just electricity but also produce heating, cooling, hot water for domestic application, and hydrogen gas as a fuel to power the fuel cell at night or during low temperature whether. Also, with the hike in electricity tariff due to high prices of fossil fuels, the proposed MGPP offers a low cost of operation due to availability of solar energy and net zero carbondioxide (CO_2) emission since its only by-product is just water.

In this work, the performance of a MGPP was investigated based on the thermodynamic and economic perspectives considering Calabar area. Further research could be done by considering solar and biomass, or solar and geothermal for the same region – Calabar. It could also be possible to reduce the turbine temperature by choosing a low temperature working fluid for the ORC in order to achieve a more efficient ORC performance.

REFERENCES

[1] Ahmadi, P., Dincer, I., and Rosen, M. A. "Exergo-environmental analyses of an integrated Organic Rankine Cycle for trigeneration", *Energy conversion and Management*. 64; 2012, 447-453.

[2] Bicer, Y., and Dincer, I. "Development of a new solar and geothermal based combined system for hydrogen production", *Solar Energy*, 127: 2016; pp. 269-284.

[3] Ozturk, M., and Dincer, I. "Thermodynamic assessment of an integrated solar power tower and coal gasification system for multigeneration purposes", *Energy Conversion and Management*, 76: 2013; pp 1061-72.

[4] Mohan, G., Dahal, S., Kumar, U., Martin, A., and Kayal, H. "Development of natural gas fired combined cycle plant for tri-generation of power, cooling and clean water using waste heat recovery: techno-economic analysis", *Energies*. 7(10), 2014; pp. 6358-6381.

[5] Al-Ali, M., and Dincer, I. "Energetic and exergetic studies of a multigenerational solar–geothermal system", *Applied Thermal Engineering*, 71(91): 2015; 16-23.

[6] Kalinci, Y., Dincer, I., and Hepbasli, A. "Energy and exergy analyses of a hybrid hydrogen energy system: a case study for Bozcaada", *International Journal Hydrogen Energy*, 42(4): 2017; pp 2492-503.

[7] Ozlu, S., and Dincer, I. "Development and analysis of a solar and wind energy based multigeneration system", *Solar Energy*, 122, 2015; 1279-1295. http://dx.doi.org/10.1016/j.solener.2015.10.035.

[8] Abam, F. I., Ogheneruona, E., Diemuodeke, E. B., Mohammed A., Olusegun, D. S., Zafar, A. K., Muhammad, I., and Muhammad, F. "Exergoeconomic and Environmental Modeling of Integrated Polygeneration Power Plant with Biomass-Based Syngas Supplemental Firing", *Energies*, 2020, 13, 6018; doi: 10.3390/en13226018

[9] Kalogirou, S. A., "Solar Energy Engineering: Processes and Systems", *Academic Press*, 2013.

[10] Khalid, F., Dincer, I., and Rosen, M. A. "Techno-economic assessment of a solar-geothermal multigeneration system for

buildings", *International Journal of Hydrogen energy*, 42(33): 2017; 21454-21462.

[11] Ni, M., Leung, M. K. H., and Leung, D. Y. C. "Electrochemistry modelling of proton exchange membrane (PEM) water electrolysis for hydrogen production", *In Proceedings of the 16th world hydrogen energy conference*, Lyon, France, 2006; 13-16.

[12] Gurau, V., Barbir, F., and Liu, H. T. "An alternative solution of a half-cell model for PEM fuel cells", *Journal of Electrochemical Society*, 147(7): 2000; 2468-77.

[13] Rashidi, J., Ifaei, P., Esfahani, I. J., Ataei, A., and Yoo, C. H. "Thermodynamic and economic studies of two new high efficient power-cooling cogeneration systems based on kalina and absorption refrigeration cycles", *Energy Convers. Manage.* 127: 2016; 170–186.

[14] Jing, Y., Li, Z., Liu, L., and Lu, S. "Exergoeconomic Assessment of Solar Absorption and Absorption – Compression Hybrid Refrigeration in Building Cooling", *Entropy*, 2018; 20(2), 130. doi:10.3390/e200 20130

[15] Oko, C. O. C., Diemuodeke, E. O., Omunakwe, N. F., and Nnamdi, E., "Design and economic analysis of a photovoltaic system: A case study", *Int. J. Renew. Energy Dev*. 1(3), 2012; 65–73.

[16] Esfahani, I. J., Lee, S., amd Yoo, C. 2015. "Evaluation and optimization of a multi-effect evaporation–absorption heat pump desalination based conventional and advanced exergy and exergoeconomic analyses", *Desalination*, 359: 2015; 92–107

[17] Dabwan, Y. N., and Mokheimer, E. M. A. "Optimal integration of linear Fresnel reflector with gas turbine cogeneration power plant", *Energy Conversion and Management*, 148, 2017; 830–843. doi: 10.1016/j.enconman.2017 .06.057

[18] Ifaei, P., Rashidi, J., and Yoo, C. "Thermoeconomic environmental analyses of a low water and consumption combined steam power plant and refrigeration chillers– Part 1: energy and economic modelling and analysis", *Energy Convers. Manage.*, 2016; 123: 610–24.

[19] Owebor, K., Oko, C. O. C., Diemuodeke, E. O., and Ogorure, O. J. "Thermoenvironmental and economic analysis of an integrated municipal waste-to-energy solid oxide fuel cell, gas-, steam-, organic fluid- and absorption refrigerat-ion cycle thermal power plants", *Applied Energy*, vol. 239, 1 April 2019; 1385-1401; doi: https://doi.org/10.1016/j.apenergy.2019.02.032